Tape casting of multilayer YAG-Nd:YAG transparent ceramics for laser applications: Study of green tapes properties

Rémy Belon, Rémy Boulesteix, Pierre-Marie Geffroy, Alexandre Maitre, Christian Sallé, Thierry Chartier

Tape casting of multilayer YAG-Nd:YAG transparent ceramics for laser applications: study of green tapes properties

Rémy Belon[1,2,3], Rémy Boulesteix[1,2*], Pierre-Marie Geffroy[1], Alexandre Maître[1,2], Christian Sallé[2,3], Thierry Chartier[1]

[1] Univ. Limoges, CNRS, IRCER, UMR 7315, F-87000 Limoges, France

[2] LCTL, IRCER, UMR 7315, F-87000 Limoges, France

[3] CILAS, F-45063 Orléans, France

(*) Author to whom the correspondence should be addressed
Univ. Limoges, CNRS, IRCER, UMR 7315, F-87000 Limoges, France
Tel.: +33 (0)5 87 50 23 45
E-mail: remy.boulesteix@unilim.fr

Abstract

In this study, the mechanical properties of ceramic green tapes elaborated by tape casting were determined. The influence of slurry formulation (*i.e.* organic content and binder-to-plasticiser volume ratio) on these properties was studied. In the studied formulation domain with polyvinyl butyral (PVB) and benzyl butyl phthalate (BBP) as binder (B) and plasticiser (P) respectively, it was shown that maximum elongation, maximum stress and Young's modulus are increased for higher organic content and B/P ratio. This work also shows the possibility to manufacture multi-layered transparent ceramics for waveguide applications by the tape casting process. In that case, a compromise has been identified between good mechanical properties and low organic content that can alter the transparency of the material.

Keywords

Transparent ceramics; tape casting; mechanical properties; waveguide

Introduction

For high demanding laser applications, amplifier media with new architectures (*i.e.* with dopant gradient) also called "composites" need to be developed. These architectures have many advantages, compared to a homogeneous component. For instance, Kracht *et al.* [1] demonstrated that a multi-layered barrel of YAG single-crystal, with increasing Nd-dopant concentration in three steps along the optical axis in the barrel, makes possible to smooth the absorption of the pumping beam, and thus to smooth the temperature and stress gradient in the barrel. This enables to increase the pumping power, and so higher output laser power can be obtained. As reported in this study, first graded components were manufactured by diffusion-bonding of single-crystals [2]. Nevertheless, diffusion-bonding is restricted to simple architectures, with plane interfaces (see examples in [3,4]). In addition, diffusion-bonding process requires a very high-quality polishing of each surfaces to be contacted and remains expensive [2]. On the contrary, ceramic processes permit to control the architecture of the final material thanks to adapted shaping processes. Ikesue and Aung [5] gives for instance some architectures of interest for laser applications that can be manufactured by ceramic processing: multi-layered, cylindrical clad-core structure, fiber clad-core, waveguide or continuous gradient. The waveguide architecture is very interesting because of its higher gain and better thermal management compared to a bulk material [6]. The waveguide geometry also permits to design photonic integrated circuit, and allows to manufacture compact laser devices [7,8]. Finally its lower laser threshold leads also to a lower power consumption [9].

In order to manufacture composite ceramics with composition gradient, several shaping methods exist, such as powders co-pressing [10–12], sequential slip casting [13–15] or tape

casting [16–18]. The latter is well-adapted to manufacture ceramics with layered architecture and good spatial resolution. So, electronic components like multilayer ceramic capacitors with alternative layers of $Zn_{0.95}Mg_{0.05}TiO_2$ of 30 µm of thickness, metallised with Ag [19] can be manufactured. Tape casting thus appears as a very promising way to manufacture transparent composite ceramics with waveguide architecture. Transparent rare-earth-doped YAG waveguides have already been manufactured [20–22]. A multilayer Yb:YAG was also elaborated by tape casting [23]. Besides, tape casting process can be used to manufacture multi-layered transparent ceramics of large size: Ter-Gabrielyan *et al.* present a three-layered Er:YAG ceramic, with a length of 62 mm, elaborated by co-casting [24]. These studies showed that tape casting is well-adapted to manufacture transparent ceramics with good laser performances.

Transparent ceramics manufacturing requires the optimization of each process step to avoid the presence of scattering centres as pores, micro-cracks, secondary phases, etc. [25]. Using tape casting as shaping method needs the elaboration of specific ceramic suspension with organic additives of high purity and a low organic content to obtain a high green density. Otherwise, green tapes showing suitable mechanical properties and without internal stresses are needed to limit deformation or micro-cracks after drying. Indeed, the slurry formulation, in particular organic content and binder/plasticiser ratio, have a large impact on the values of internal stresses in the green tape during and after the drying stage [26]. The creation of micro-cracks in the green tape is directly correlated to the formulation of the slurry. A few works studied the mechanical properties of the green tapes as a function of the slurry formulation, mainly for aqueous systems. Burnfield and Peterson [27] observed that the maximum stress increases with the binder (hydroxyethylcellulose) content. The same authors have shown that the maximum stress decreases while maximum elongation increases when plasticiser content increases. Doreau *et al.* [28] observed an opposite trend concerning an acrylic emulsion used as binder. Indeed, in this case the maximum stress decreases and the maximum elongation

increases when the binder content increases. Khamkasem *et al.* [29] studied the influence of the binder/plasticiser (B/P) ratio, and showed that the maximum stress increases and the maximum elongation decreases when the ratio B/P increases (so when the binder content increases). Albano *et al.* [30] reported that the maximum stress increases with the binder content (range from 5 to 7 wt.%) and the B/P ratio (0.7 to 1.5). According to the same authors, the maximum elongation increases when the ratio B/P decreases. Chartier *et al.* [31] observed that maximum elongation decreases and maximum stress increases when the ratio B/P increases. Finally, all these studies concerning tape casting showed that the formulation of the slurries controls the mechanical properties of the green tapes.

Consequently, this paper will be focused on the implementation of a shaping process by tape casting for YAG-Nd:YAG transparent composite ceramic with waveguide architecture. This latter architecture consists in a thin layer of Nd:YAG (around 150 µm thick) embedded in an undoped YAG matrix. Moreover this paper will be focused on the mechanical properties of the green tapes. More particularly, two parameters will be investigated: the total organic content and the binder-to-plasticiser volume ratio. The final objective will be twofold: i) to obtain green tapes having good mechanical properties to avoid micro-cracks in the final material; ii) to limit the organic content in order to ease the debinding step and to limit the contamination by residual carbon and/or impurities.

1. Experimental procedure

1.1. Elaboration and tape casting of the slurries

Al_2O_3 powder (Baïkowski, France) and Y_2O_3 powder (Solvay, Belgium) with high purity (> 99.99 %) were used as starting materials. These powders were weighted according to stoichiometry ratio to obtain $Y_3Al_5O_{12}$ (*i.e.* undoped YAG). The powders were mixed with 4-hydroxybenzoic acid as dispersant (3 wt.%), in an azeotropic mixture of methyl ethyl ketone

(MEK) and ethanol (60 vol.% of MEK + 40 vol.% of ethanol), with a ceramic solid loading of 25 vol.%, and ball milled during 4 h with alumina balls. Then, binder and plasticiser were added to the slurry, which was homogenised by milling for 20 h. Polyvinyl butyral (PVB) and benzyl butyl phthalate (BBP) were used as binder and plasticiser, respectively. Organic additives (dispersant, binder and plasticiser) content (X = additives volume/[additives + ceramic powder volume]) was varied in a range of 40 to 50 vol.%. Binder-to-plasticiser volume ratio (B/P = binder volume/plasticiser volume) was varied in a range of 0.3 to 1. Formulations were named as follow: [Organic content]-[Volume ratio B/P]. For instance, the formulation noted "50-1" corresponds to the ceramic suspension with an organic content of 50 vol.% and a ratio B/P of 1. Slurries were tape-cast on a Mylar film substrate using a double doctor blade system. The speed of the doctor blade was 0.90 $cm.s^{-1}$ and the height between the blades and the Mylar film was 300 µm. The thickness of the green tapes was about 100 µm after drying.

1.2. Mechanical characterisations of green tapes

Mechanical properties of the green tapes were evaluated by two methods. First, the maximum elongation of green tape before cracking was measured by a method reported by Mistler [32]. The green tapes were rolled on cylinders of different diameters, successively from the biggest to the smallest diameter, until cracks appeared on the green tape. The maximum elongation can be calculated with the following equation:

$$\varepsilon_c\ (\%) = [(r+e)/r - 1] \times 100 \qquad \text{Eq. 1}$$

where ε_c is the maximum elongation, r the smallest cylinder radius without cracks in the tape, and e the green tape thickness. Cylinders of five different radii were used for tapes thickness of 100 µm: 50, 30, 20, 10, and 5 mm, corresponding to maximum elongation of 0.2, 0.33, 0.5, 1 and 2 %, respectively.

Secondly, tensile tests were carried out on dog-bone shaped specimens (**Figure 1**) cut parallel to the casting direction by laser cutting. A Lloyd Instrument EZ20 apparatus equipped with a 100 N load cell was used. The traverse speed was set to 0.5 $mm.min^{-1}$.

The tensile strength σ_m (maximum stress) and the maximum elongation ε_m (elongation at rupture) were determined from the stress-strain curve of the green tape (**Figure 2**). Indeed, the curve can be dissociated in two characteristic domains:

i) the first one, corresponding to low deformation (linear part), is related to the elastic deformation,

ii) the second one is related to the plastic deformation, until the rupture.

The elastic deformation can be evaluated from the Hooke's law [33], only valid for low deformation:

$$\sigma = E \times \varepsilon \qquad \text{Eq. 2}$$

According to Eq. 2, the Young's modulus E was determined from the slope of the linear part of the curve. Five samples were tested for each composition, and the average value of σ_m, ε_m and E was determined.

1.3. Manufacturing of composite ceramic with a waveguide architecture

For the elaboration of the multi-layered ceramics, two types of slurries were prepared: a first slurry composed of Y_2O_3 and Al_2O_3 powders mixed with suitable ratio for YAG composition ($Y_3Al_5O_{12}$), and a second slurry composed of Y_2O_3, Al_2O_3 and Nd_2O_3 powders mixed with suitable ratio for Nd:YAG composition ($Nd_{0.03}Y_{2.97}Al_5O_{12}$, or 1 at.% Nd:YAG). Nd_2O_3 powder of high purity (> 99.99 %, Auer-Remy, Germany) was used as dopant source. The properties (particle-size distribution and rheological behaviour) of Nd:YAG slurry were

compared to that of pure YAG slurry. No significant differences were observed. Then, it was assumed that adding Nd_2O_3 doesn't modify the green tapes properties. Tetraethylorthosilicate (TEOS) was added as sintering aid, in the amount of 0.24 wt.% (corresponding to 0.07 wt.% of SiO_2). Considering the low content added to the slurries, it was also assumed that TEOS doesn't modify the slurries and green tapes properties. Both slurries were tape-cast in the conditions described in the previous paragraph.

After drying, disks of 30 mm diameter were cut into the green tapes. 42 disks were stacked (20 undoped disks + 2 doped disks + 20 undoped disks) in a die and laminated at 95 °C under 35 MPa, for 5 min. Debinding was carried out under air at 650 °C, during 1 h. Then, sintering was achieved in a tungsten mesh-heated furnace at 1740 °C during 20 h under vacuum. Microstructure observations were carried out by using conventional Scanning Electron Microscopy (LEO 1530VP, Zeiss, Germany, and FEI Quanta 450, Thermo Fisher Scientific, USA). Neodymium repartition in the sample was characterised by fluorescence microscopy and its concentration profile was measured by electron probe microanalysis (SX 100, CAMECA, France).

2. Results and discussion

2.1. Green tapes characterisation

Figure 3 shows the microstructure of a green tape, after debinding at 650 °C. The two powders (yttria circled in green and alumina circled in blue) appear to be well dispersed.

Figure 4 shows the impact of binder-plasticiser volume ratio and organic content on the maximum elongation before cracking of the green tapes (cylinders method). From this figure, three characteristic domains can be observed:

- the area numbered I corresponds to the formulations with a maximum elongation higher than 2 %. This formulation domain with high elongation is suitable to prevent eventual cracks after drying, cutting and thermo-lamination;
- the area numbered III corresponds to a maximum elongation lower than 0.2 % (50-mm-radius cylinder). In this formulation domain, some cracks appear in green tapes during drying, and the green tapes are not flexible and not easily to handle for the lamination process;
- the intermediate area numbered II corresponds to a maximum elongation between 0.2 and 2 %.

According to the results of **Figure 4**, mechanical properties of the green tapes quickly decrease out of the area I, and a slight variation of the formulation leads to a large variation of mechanical properties of the green tapes. As reported on the **Figure 4**, green tapes have no defects in area I (photo c) whereas cracks appear rapidly out of this domain (area II and III illustrated by photo a and b).

Green tapes properties can be interpreted as below: (1) when the binder-to-plasticiser (B/P) ratio is too low (bottom of the graph in **Figure 4**), there is not enough binder to ensure the cohesion of the tapes, so the latter disintegrates during drying. (2) Conversely, if B/P ratio is too high (more binder and less plasticiser, top of the graph), tapes are too stiff, and they cannot deform during drying, leading to the appearance of cracks (**Figure 4 photo a**). (3) When organic content is too low (left of the graph in **Figure 4 photo a**), cracks appear whatever the B/P ratio because there is not enough organics to ensure the cohesion of the tapes. (4) Green tapes with good mechanical properties and thus with no cracks are obtained for suitable B/P ratio (around 0.7) and a minimum organic content of about 40%.

In order to further characterise the mechanical properties of green tapes, tensile tests were carried out with green tapes having a maximum elongation larger than 2 %. The relative density of the green tapes after debinding was also measured for each formulation. For this purpose, disk samples were cut in tapes of each formulation. Samples volume V was geometrically determined. Finally, the samples were debinded and the mass m of each debinded sample was measured. So, the density ρ of each tape can be calculated ($\rho = m/V$), and the relative density was given according to the YAG theoretical density ($\rho_{YAG} = 4.55$ g.cm^{-3}). The relative densities of the green tapes are similar in the formulation range of this study (average of 35 % with a standard deviation of 0.8 %). Then, it was assumed that the impact of the relative density on the mechanical properties of the green tapes is not significant in this work. Obtained values (*i.e.* maximum elongation ε_m, Young's modulus E, and maximum strength σ_m) from stress-strain curves as illustrated in **Figure 2** were reported in **Figure 5**.

The general trend assessed from the **Figure 5 graph a** is that maximum elongation increases with the organic content (**Figure 5 graph a**). This is an expected evolution, since the organic content is favourable to a ductile behaviour of the green tape with a larger strength. Also, maximum elongation increases with ratio B/P (*i.e.* when the amount of plasticiser decreases). This is unusual in comparison with data reported in the literature [27,29,30]. The ratios B/P (<1) of the formulations studied in this work are lower, compared with ratios close to the unity reported in the literature. This leads likely to a lower ductility and strength of our green tapes (< 1.8 MPa, compared with strength > 1.5 MPa in the literature previously cited).

Young's modulus increases when B/P ratio and organic content increase (**Figure 5 graph b**). Higher organic content (50 vol.%) leads to stiffer green tapes, as expected. However, the green tape noted 40-0.7 (40 vol.% organic content - binder/plasticiser = 0.7) with the lower organic content, shows highest Young's modulus. This can be explained because the high ceramic content in this case leads to a fragile behaviour of the green tape with low relaxation of internal

stresses and an increase of Young's modulus of the green tape. This behaviour has already been observed for particulate-filled polymer composites [34,35].

The impact of B/P ratio and organic content on maximum stress before rupture is still negligible when organic content is under 45 vol.% (**Figure 5 graph c**). Nevertheless, the maximum stress before rupture increases with higher organic content (50 vol.%) and a higher ratio B/P (≥ 0.7). For instance, the maximum stress is almost doubled when B/P ratio increases from 0.4 to 1 (organic content of 50 vol.%). Indeed, the B/P ratio and the organic content of the suspension imposes mechanical behaviour evolution of the green tape, from fragile to ductile behaviour, as observed by Campbell [36] in composite materials.

2.2. Manufacturing and characterisation of composite transparent ceramic

The production of transparent ceramics needs to prohibit the formation of microstructural defects (*e.g.* secondary phase, (micro-)cracks) during ceramic process. Besides, manufacturing of transparent ceramics requires a very high relative density (> 99,9 %) of the sintered parts. This involves to obtain green tapes with a high relative density but also to limit the organic content in the slurry formulation. In this respect, formulation with the lowest organic content allowing to manufacture green tapes without defects (i.e. organic content close to 40 vol.% with B/P ratio of 0.7 according to **Figure 4**) was selected.

The microstructure of the debinded multi-layered material is shown on **Figure 6**. No defects were detected between the layers, showing that the lamination step is well controlled. Despite the low relative density of the green tapes (about 35 %), the relative density of the sample after thermo-lamination is about 45 %. So thermo-lamination leads to a better packing of the particles.

After sintering, a transparent ceramic (**Figure 7a**) is obtained. **Figure 7b** shows a cross section of the sintered composite material, with the visible thin Nd-doped layer in the middle. As shown on the **Figure 7c**, the doped layer can be seen by backscattered electron imaging. Its thickness

is about 135 µm, for a green thickness of 200 µm. No cracks or delamination were observed at the interfaces, so co-sintering of doped and undoped layers was going well. Some intragranular pores (small circular black spots, **Figure 7c**) could not be eliminated during sintering. Also, a few contents of alumina particles (irregular black spots, **Figure 7c**) are remaining in the sample. These particles should result from a slight deviation of the initial stoichiometry (*i.e.* of the ideal Y/Al ratio of 0.6).

Concerning the optical quality of the sample, the transmission spectrum is shown on **Figure 8.** The Nd^{3+} absorption peaks are weak, due to the low thickness of the Nd-doped layer. The transmittance is 54.2 % and 52.1 % at 1064 nm and 400 nm respectively, for a total sample thickness of 3,8 mm. This is not as high as the theoretical transmittance of YAG (84 %), and this work needs some improvements, more particularly on the microstructural homogeneity of the sample.

One can see on the **Figure 9a** the micrograph of a cross-section of multi-layered YAG/Nd:YAG ceramic obtained by fluorescence microscopy (imaging at 1064 nm, with 808 nm excitation). According to this figure, Nd^{3+} detected by its strong luminescence at 1064 nm is located in a central layer in the composite as expected. The profile of neodymium concentration was characterised more precisely and quantitatively by electron probe microanalysis (**Figure 9b**). Nd^{3+} concentration is given as an atomic percentage regarding to the yttrium content. The concentration in the doped layer is about 1 at.%, as expected. The profile also reveals that Nd^{3+} has diffused during co-sintering over approximately 50 µm from the initial interface. This value is in the same order of that observed by Bonnet *et al.* that used similar co-sintering conditions [13]. Results reported in **Figure 9** show that tape casting is well-adapted to control the architecture (dopant gradient) of transparent ceramics.

3. Conclusions

This work shows that tape casting process is an interesting method for manufacturing multi-layered YAG-based transparent ceramics. In this way, two points needed specific attention.

The first one is related to the mechanical properties of the green tapes. The control of the slurry formulation and the mechanical properties of the green tapes are critical parameters to obtain ceramics without defects. To obtain a green tape easy to handle (*i.e.* with a maximum strength and strain high enough), the binder and plasticiser contents are key parameters to control.

The second key parameter is the organic content of the sample. A low organic content is needed to ease the debinding step, and avoid defects creation during this treatment. Besides, formulations with less organic additives limit the chemical impurities content in the material. Finally, green tapes with a maximum strength of 1.14 MPa and a maximum elongation of 1.5 % can be manufactured, stacked, laminated and sintered, to obtain a transparent composite ceramic.

Thus, tape casting process is well-adapted to manufacture multilayer transparent ceramics, with a complex and controlled architecture, and which could be used as laser components.

Acknowledgements

We are thankful to Alain Brenier, from the Institut Lumière Matière of Lyon (France), who carried out the fluorescence microscopy characterisations and to Eric Leroy, from Institut de Chimie et des Matériaux Paris-Est (France) who performed electron probe microanalysis. The authors are also grateful to ANRT for financial support (Grant number 2015/1062).

Bibliography

[1] D. Kracht, R. Wilhelm, M. Frede, K. Dupré, L. Ackermann, 407 W end-pumped multi-segmented Nd: YAG laser, Opt. Express. 13 (2005) 10140–10144.

[2] H.-C. Lee, P.L. Brownlie, H.E. Meissner, E.C. Rea, Jr., Diffusion-bonded composites of YAG single crystals, in: H.E. Bennett, L.L. Chase, A.H. Guenther, B.E. Newnam, M.J. Soileau (Eds.), 1992: pp. 2–10. doi:10.1117/12.60125.

[3] H.E. Meissner, Composites made from single crystal substances, US5441803A, 1995. https://patents.google.com/patent/US5441803A/en (accessed December 10, 2018).

[4] H.E. Meissner, Composite optical and electro-optical devices, US5846638A, 1998. https://patents.google.com/patent/US5846638A/en (accessed December 10, 2018).

[5] A. Ikesue, Y.L. Aung, Synthesis and Performance of Advanced Ceramic Lasers, J. Am. Ceram. Soc. 89 (2006) 1936–1944. doi:10.1111/j.1551-2916.2006.01043.x.

[6] C. Grivas, Optically pumped planar waveguide lasers, Part I: Fundamentals and fabrication techniques, Prog. Quantum Electron. 35 (2011) 159–239. doi:10.1016/j.pquantelec.2011.05.002.

[7] M.C. Estevez, M. Alvarez, L.M. Lechuga, Integrated optical devices for lab-on-a-chip biosensing applications, Laser Photonics Rev. 6 (2012) 463–487. doi:10.1002/lpor.201100025.

[8] C.L. Bonner, C.T.A. Brown, D.P. Shepherd, W.A. Clarkson, A.C. Tropper, D.C. Hanna, B. Ferrand, Diode-bar end-pumped high-power Nd:Y_3Al_5O_12 planar waveguide laser, Opt. Lett. 23 (1998) 942. doi:10.1364/OL.23.000942.

[9] J.I. Mackenzie, Dielectric Solid-State Planar Waveguide Lasers: A Review, IEEE J. Sel. Top. Quantum Electron. 13 (2007) 626–637. doi:10.1109/JSTQE.2007.897184.

[10] L. Sun, A. Sneller, P. Kwon, Fabrication of alumina/zirconia functionally graded material: From optimization of processing parameters to phenomenological constitutive models, Mater. Sci. Eng. A. 488 (2008) 31–38. doi:10.1016/j.msea.2007.10.044.

[11] T. Liu, X. Wang, X. Zhang, X. Gao, L. Li, J. Yu, X. Yin, A limiting current oxygen sensor prepared by a co-pressing and co-sintering technique, Sens. Actuators B Chem. 277 (2018) 216–223. doi:10.1016/j.snb.2018.09.007.

[12] V.V. Osipov, V.A. Shitov, V.I. Solomonov, K.E. Lukyashin, A.V. Spirina, R.N. Maksimov, Composite Nd:YAG/Cr4+:YAG transparent ceramics for thin disk lasers, Ceram. Int. 41 (2015) 13277–13280. doi:10.1016/j.ceramint.2015.07.109.

[13] L. Bonnet, R. Boulesteix, A. Maître, C. Sallé, V. Couderc, A. Brenier, Manufacturing issues and optical properties of rare-earth (Y, Lu, Sc, Nd) aluminate garnets composite transparent ceramics, Opt. Mater. 50 (2015) 2–10. doi:10.1016/j.optmat.2015.04.050.

[14] J.S. Moya, A.J. Sánchez-Herencia, J. Requena, R. Moreno, Functionally gradient ceramics by sequential slip casting, Mater. Lett. 14 (1992) 333–335. doi:10.1016/0167-577X(92)90048-O.

[15] J. Chu, H. Ishibashi, K. Hayashi, H. Takebe, K. Morinaga, Slip Casting of Continuous Functionally Gradient Material, J. Ceram. Soc. Jpn. 101 (1993) 841–844. doi:10.2109/jcersj.101.841.

[16] J. Hostaša, A. Piancastelli, G. Toci, M. Vannini, V. Biasini, Transparent layered YAG ceramics with structured Yb doping produced via tape casting, Opt. Mater. 65 (2017) 21–27. doi:10.1016/j.optmat.2016.09.057.

[17] P.Z. Cai, D.J. Green, G.L. Messing, Constrained Densification of Alumina/Zirconia Hybrid Laminates, I: Experimental Observations of Processing Defects, J. Am. Ceram. Soc. 80 (1997) 1929–1939. doi:10.1111/j.1151-2916.1997.tb03075.x.

[18] T. Chartier, T. Rouxel, Tape-cast alumina-zirconia laminates: Processing and mechanical properties, J. Eur. Ceram. Soc. 17 (1997) 299–308. doi:10.1016/S0955-2219(96)00131-8.

[19] Y.-C. Lee, Investigation of thin film end-termination on multilayer ceramic capacitors, Mater. Chem. Phys. 110 (2008) 100–105. doi:10.1016/j.matchemphys.2008.01.025.

[20] L. Ge, J. Li, Z. Zhou, H. Qu, M. Dong, Y. Zhu, T. Xie, W. Li, M. Chen, H. Kou, Y. Shi, Y. Pan, X. Feng, J. Guo, Fabrication of composite YAG/Nd:YAG/YAG transparent ceramics for planar waveguide laser, Opt. Mater. Express. 4 (2014) 1042–1049. doi:10.1364/OME.4.001042.

[21] C. Ma, F. Tang, H. Lin, W. Chen, G. Zhang, Y. Cao, W. Wang, X. Yuan, Z. Dai, Fabrication and planar waveguide laser behavior of YAG/Nd:YAG/YAG composite ceramics by tape casting, J. Alloys Compd. 640 (2015) 317–320. doi:10.1016/j.jallcom.2015.03.246.

[22] C. Wang, W. Li, C. Yang, D. Bai, J. Li, L. Ge, Y. Pan, H. Zeng, Ceramic planar waveguide laser of non-aqueous tape casting fabricated YAG/Yb:YAG/YAG, Sci. Rep. 6 (2016) 31289. doi:10.1038/srep31289.

[23] J. Hostaša, A. Piancastelli, G. Toci, M. Vannini, V. Biasini, Transparent layered YAG ceramics with structured Yb doping produced via tape casting, Opt. Mater. (n.d.). doi:10.1016/j.optmat.2016.09.057.

[24] N. Ter-Gabrielyan, L.D. Merkle, E.R. Kupp, G.L. Messing, M. Dubinskii, Efficient resonantly pumped tape cast composite ceramic Er:YAG laser at 1645 nm, Opt. Lett. 35 (2010) 922–924. doi:10.1364/OL.35.000922.

[25] R. Apetz, M.P.B. van Bruggen, Transparent Alumina: A Light-Scattering Model, J. Am. Ceram. Soc. 86 (n.d.) 480–486. doi:10.1111/j.1151-2916.2003.tb03325.x.

[26] J. Kiennemann, T. Chartier, C. Pagnoux, J.F. Baumard, M. Huger, J.M. Lamérant, Drying mechanisms and stress development in aqueous alumina tape casting, J. Eur. Ceram. Soc. 25 (2005) 1551–1564. doi:10.1016/j.jeurceramsoc.2004.05.028.

[27] K.E. Burnfield, B.C. Peterson, Cellulose ethers in tape casting formulation, in: Form. Technol. Ceram., American Ceramic Society, J. Michael Cima, 1992: pp. 191–196.

[28] F. Doreau, G. Tarì, M. Guedes, T. Chartier, C. Pagnoux, J.M.F. Ferreira, Mechanical and lamination properties of alumina green tapes obtained by aqueous tape-casting, J. Eur. Ceram. Soc. 19 (1999) 2867–2873. doi:10.1016/S0955-2219(99)00052-7.

[29] C. Khamkasem, A. Chaijaruwanich, Effect of Binder/Plasticizer Ratios in Aqueous-Based Tape Casting on Mechanical Properties of Bovine Hydroxyapatite Tape, Ferroelectrics. 455 (2013) 129–135. doi:10.1080/00150193.2013.845488.

[30] M.P. Albano, L.B. Garrido, Aqueous tape casting of yttria stabilized zirconia, Mater. Sci. Eng. A. 420 (2006) 171–178. doi:10.1016/j.msea.2006.01.059.

[31] T. Chartier, A. Bruneau, Aqueous tape casting of alumina substrates, J. Eur. Ceram. Soc. 12 (1993) 243–247. doi:10.1016/0955-2219(93)90098-C.

[32] R.E. Mistler, E.R. Twiname, Tape Casting, theory and practice, The American Ceramic Society, Westerville, Ohio, 2000.

[33] M.F. Ashby, D.R.H. Jones, Engineering materials 1 An introduction to their properties and applications, Oxford : New York : Pergamon Press. 1980., 1980. http://ezproxy.unilim.fr/login?url=https://search.ebscohost.com/login.aspx?direct=true&db=cat06519a&AN=cbu.164254&lang=fr&site=eds-live.

[34] R. Rothon, Particulate-filled Polymer Composites, iSmithers Rapra Publishing, 2003.

[35] S. Ahmed, F.R. Jones, A review of particulate reinforcement theories for polymer composites, J. Mater. Sci. 25 (1990) 4933–4942. doi:10.1007/BF00580110.

[36] F.C. Campbell, Structural composite materials, ASM International, Materials Park, Ohio, 2010.

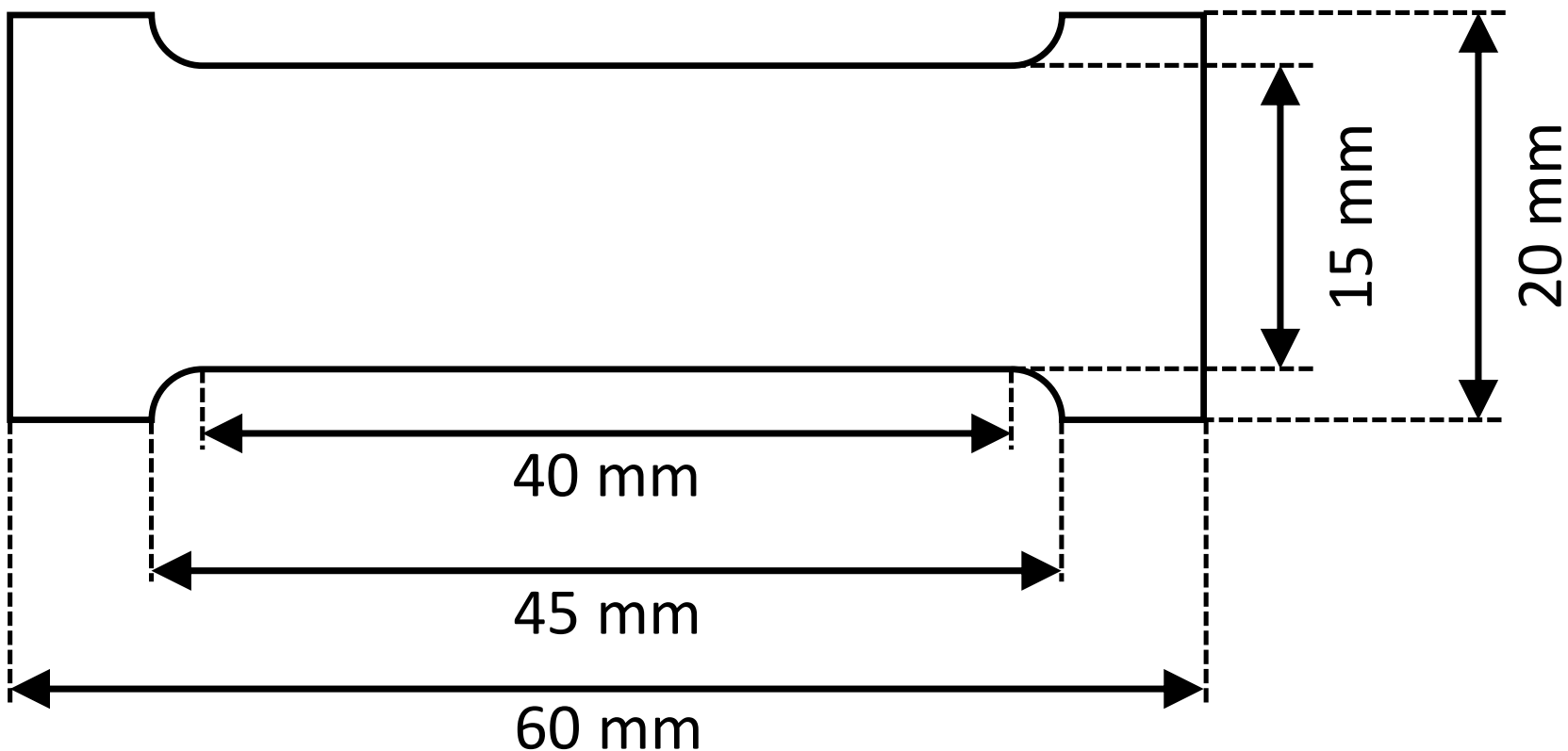
15 mm
20 mm
40 mm
45 mm
60 mm

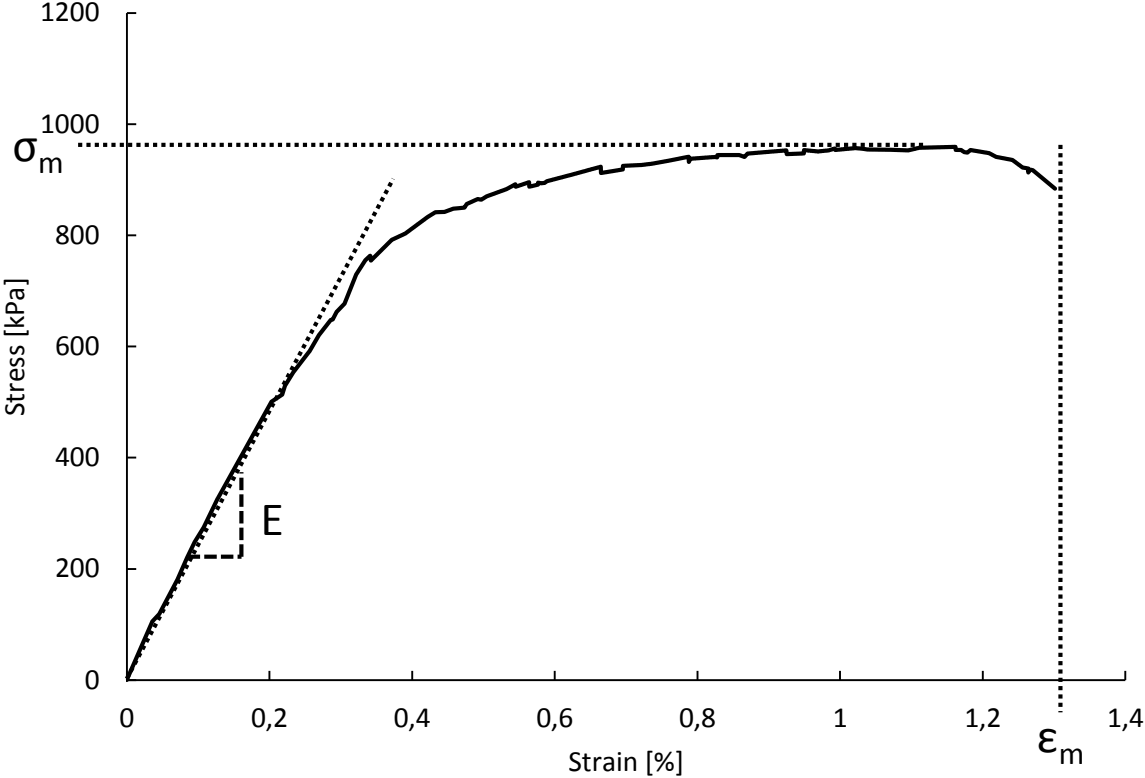
1200
1000
800
600
400
200
0
σm
Stress [kPa]
E
0
0,2
0,4
0,6
0,8
1
1,2
1,4
εm
Strain [%]

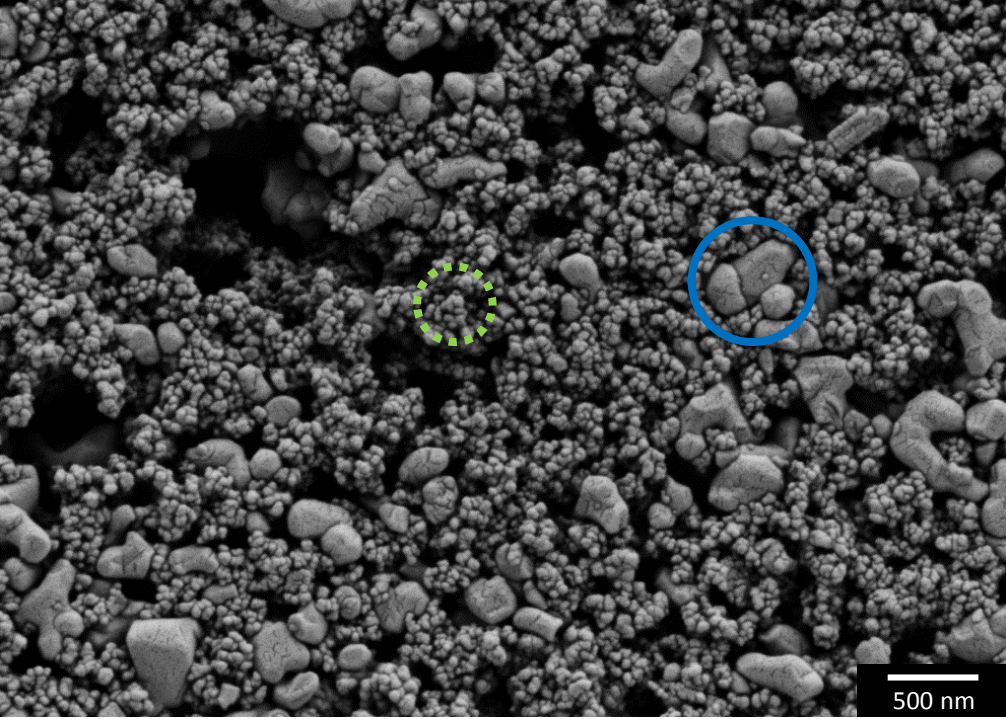
500 nm

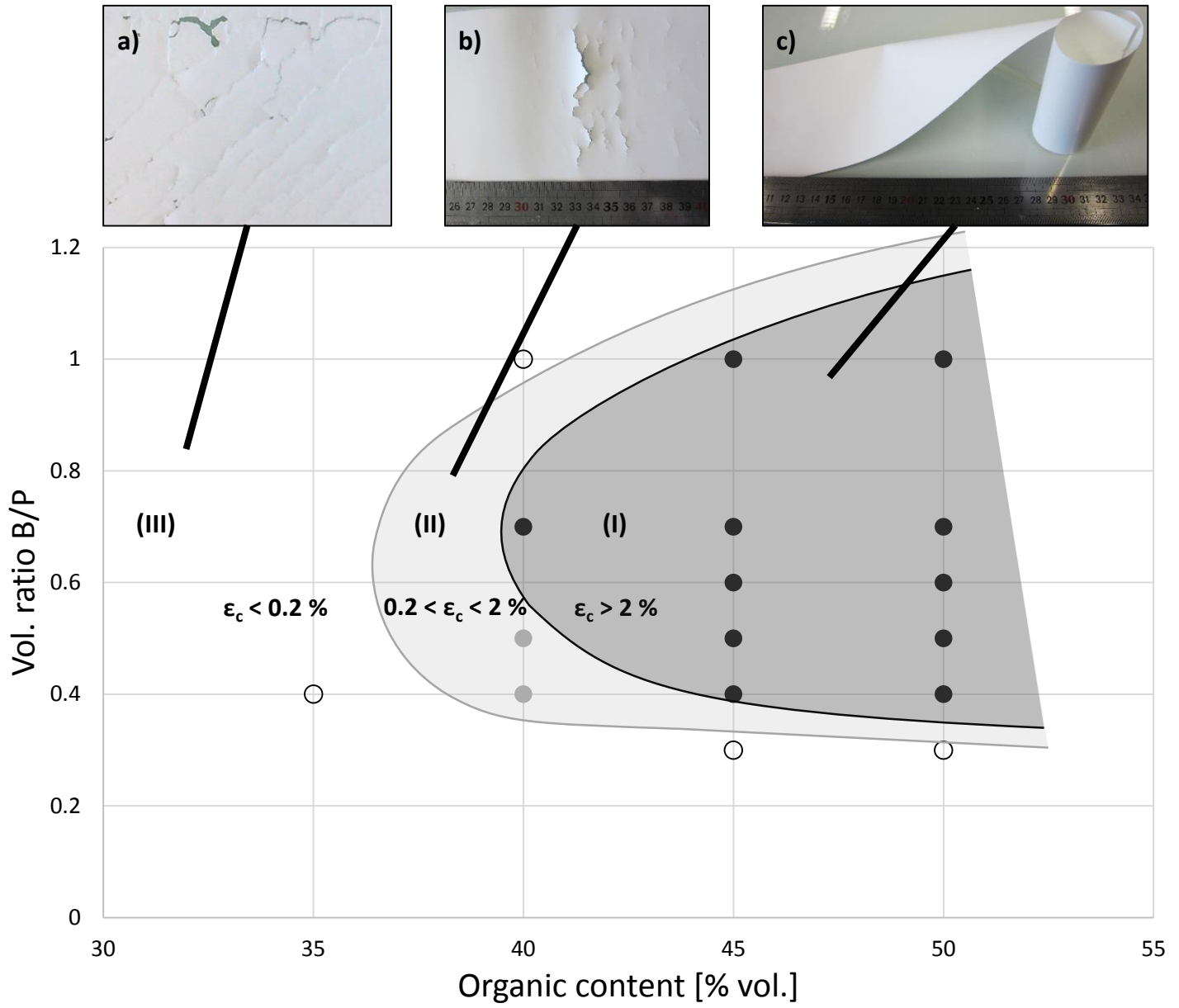
a)
b)
c)
1.2
1
0.8
0.6
0.4
0.2
0
Vol. ratio B/P
(III)
(II)
(I)
$\varepsilon_c < 0.2$ %
$0.2 < \varepsilon_c < 2$ %
$\varepsilon_c > 2$ %
30
35
40
45
50
55
Organic content [% vol.]

a)

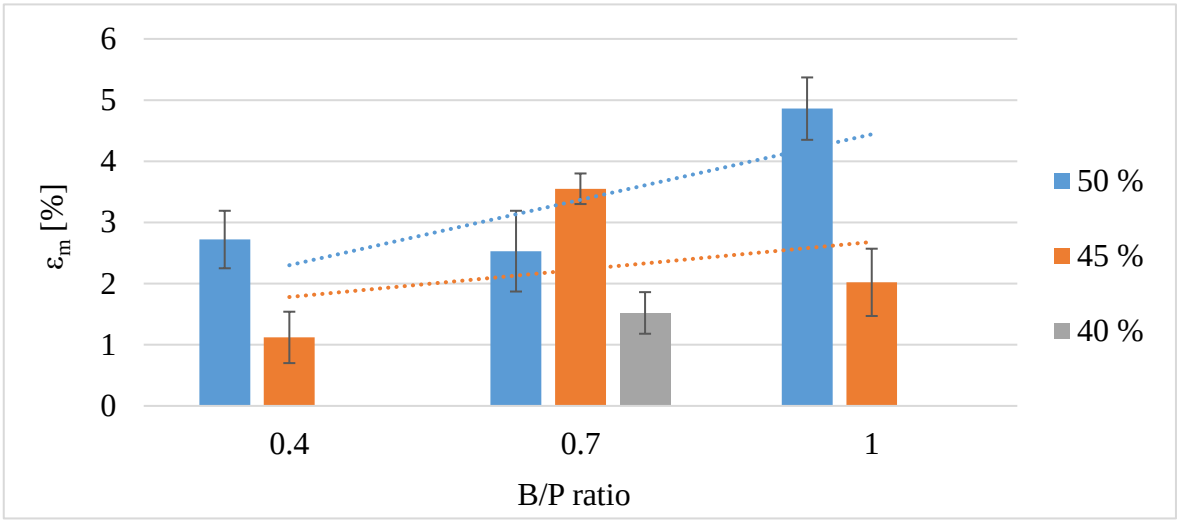
6
5
4
3
2
1
0
εm [%]
0.4
0.7
1
B/P ratio
50 %
45 %
40 %

b)

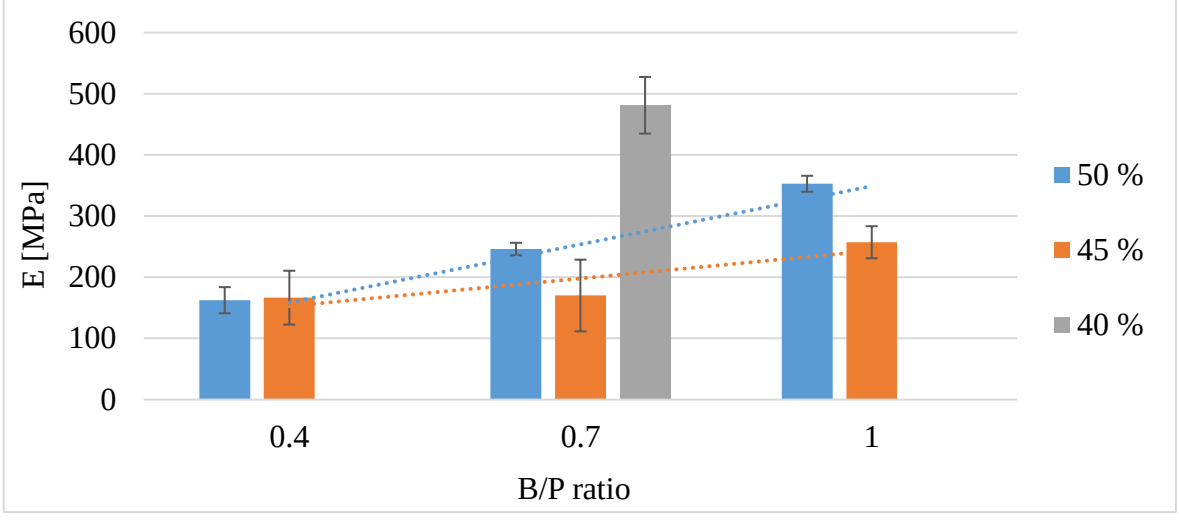
600
500
400
300
200
100
0
E [MPa]
0.4
0.7
1
B/P ratio
50 %
45 %
40 %

c)

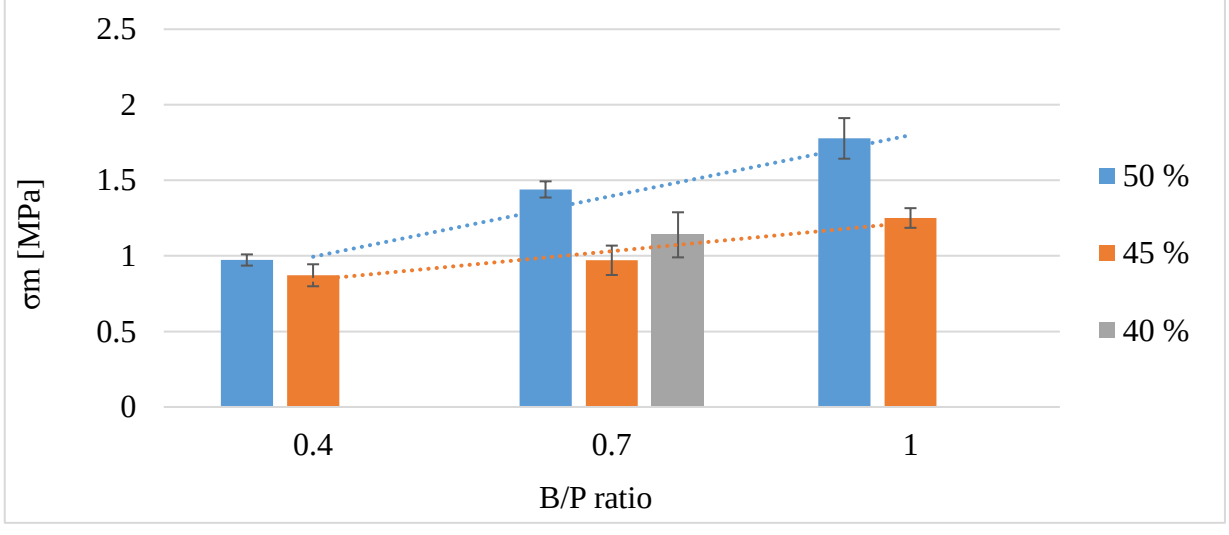
2.5
2
1.5
1
0.5
0
σm [MPa]
0.4
0.7
1
B/P ratio
50 %
45 %
40 %

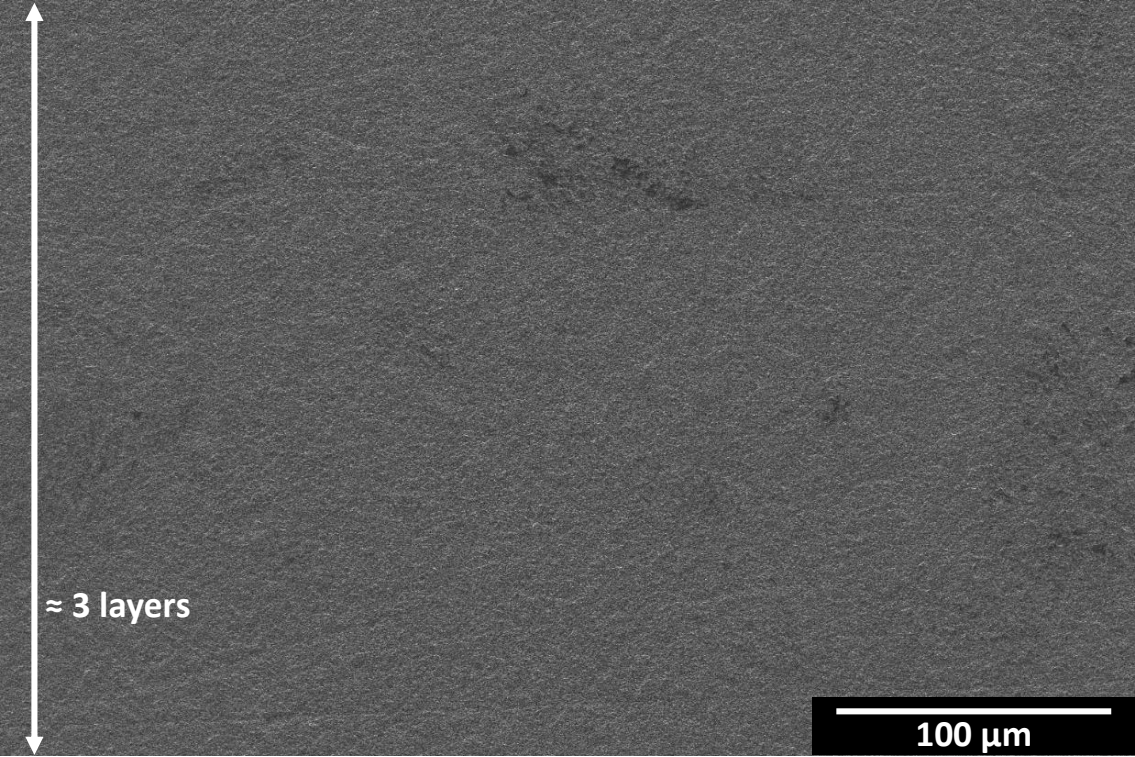
≈ 3 layers
100 µm

a)

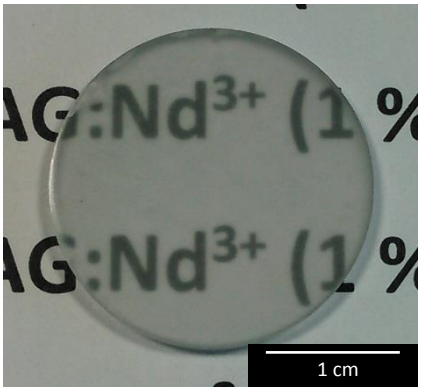
AG:Nd3+ (1 %
AG:Nd3+ (1 %
1 cm

b)

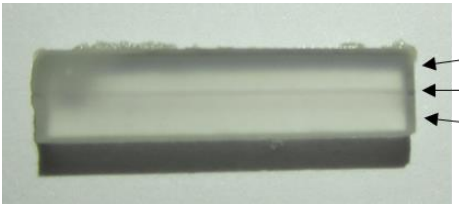
YAG
Nd:YAG layer
YAG

c)

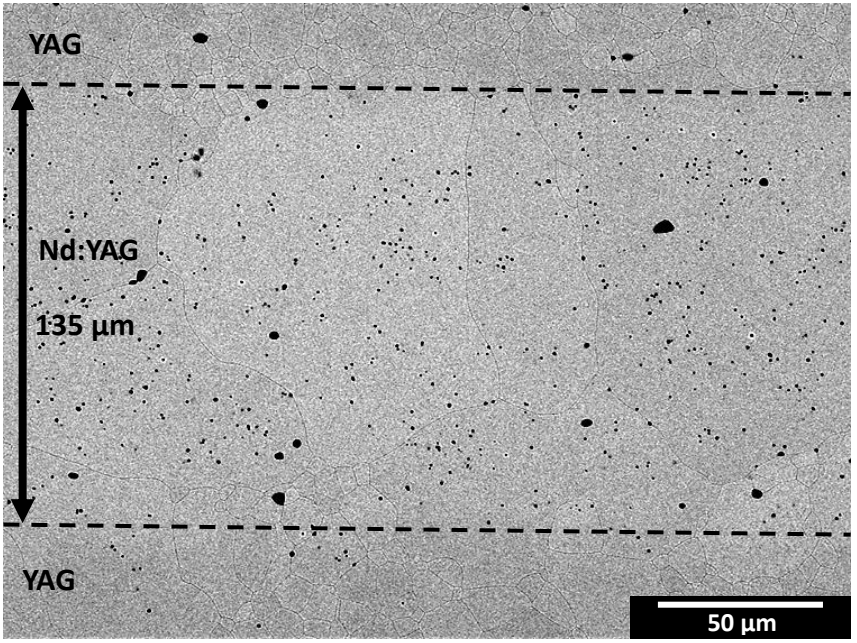
YAG
Nd:YAG
135 µm
YAG
50 µm

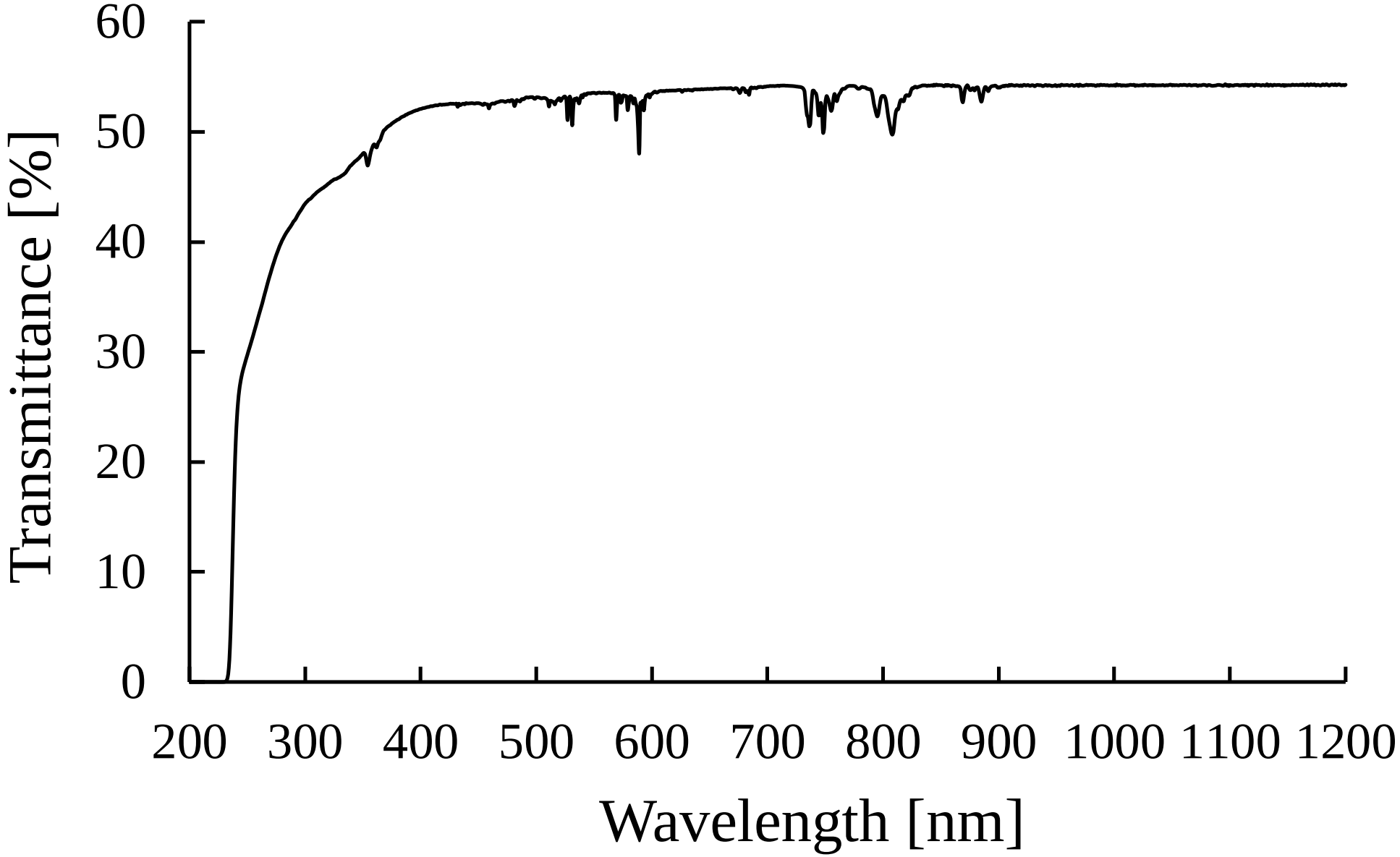
Transmittance [%]
60
50
40
30
20
10
0
200
300
400
500
600
700
800
900
1000
1100
1200
Wavelength [nm]

a)

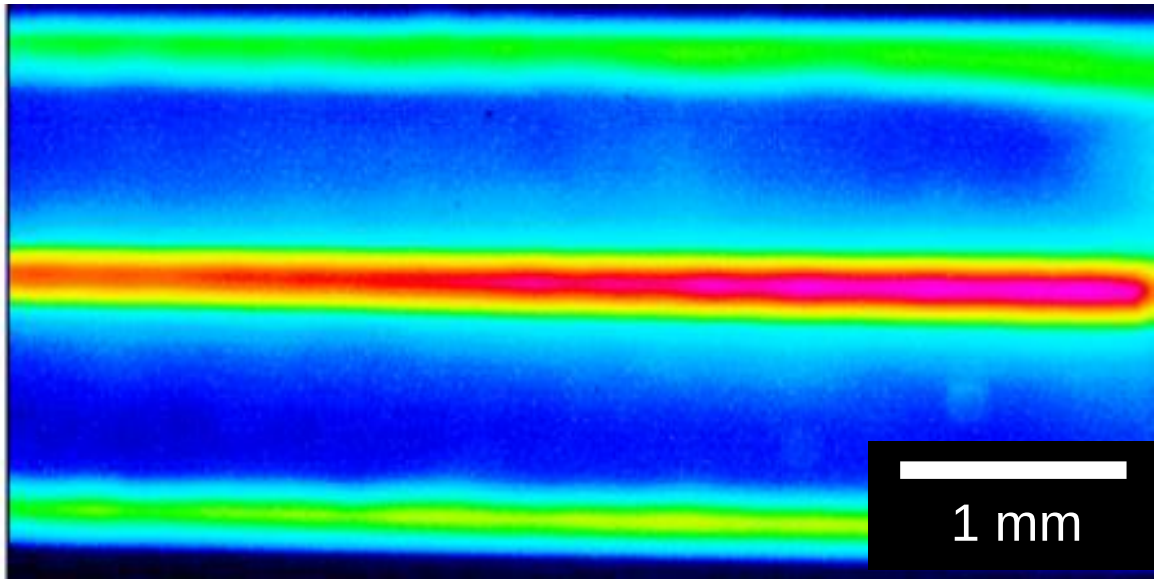
1 mm

b)

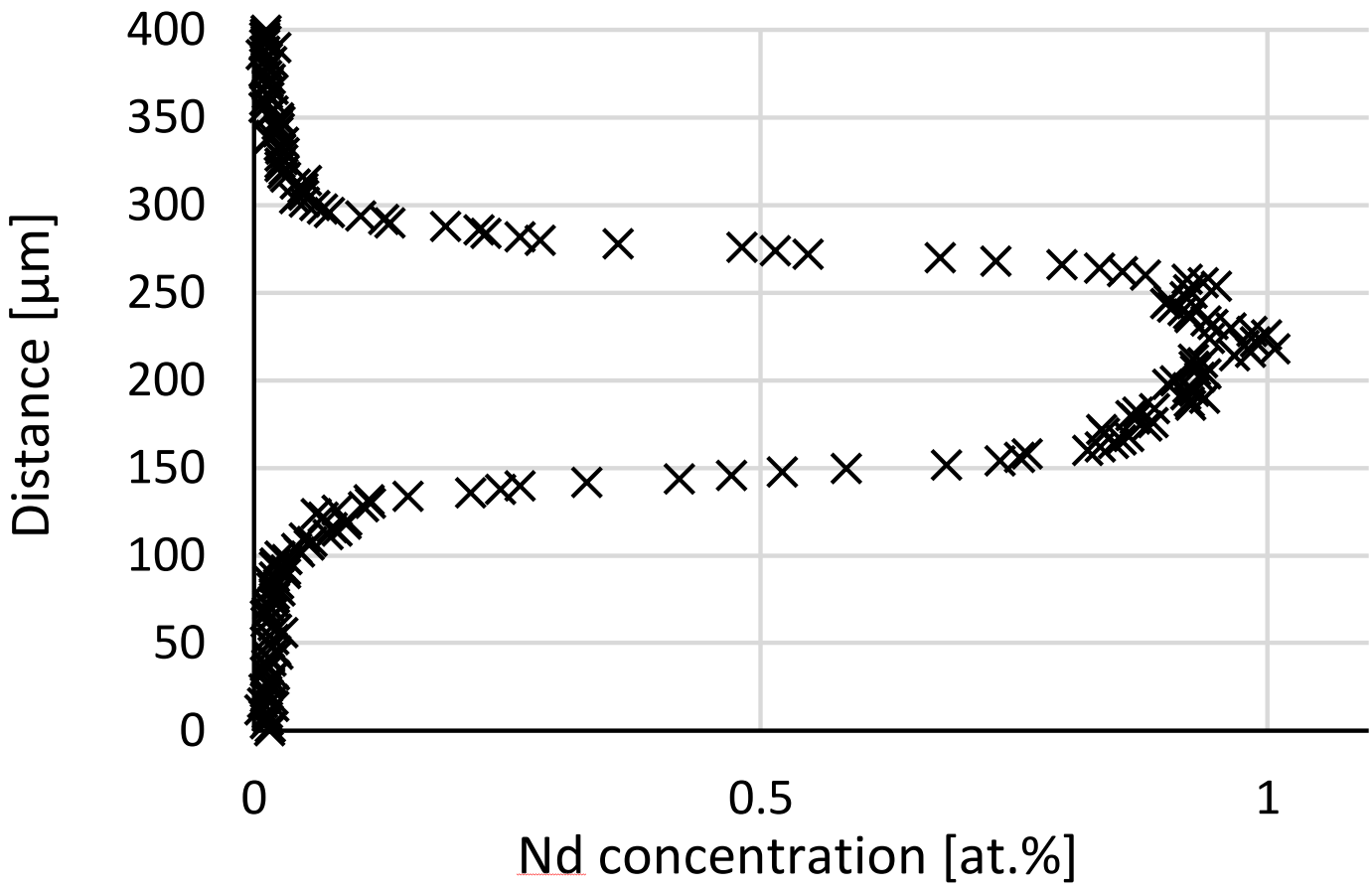
400
350
300
250
200
150
100
50
0
Distance [µm]
0
0.5
1
Nd concentration [at.%]